Silicon Solar Cell Light-Trapping Using Defect Mode Photonic Crystals

Kelsey A. Whitesell*[a], Dennis M. Callahan[a], Harry Atwater[a]
[a]Thomas J. Watson Lab. of Applied Physics, MS 128-95, California Institute of Technology, Pasadena, CA USA 91125

ABSTRACT

Nanostructured active or absorbing layers of solar cells, including photonic crystals and wire arrays, have been increasingly explored as potential options to enhance performance of thin film solar cells because of their unique ability to control light. We show that 2D photonic crystals can improve light trapping by an enhanced density of optical states and improved incoupling, and demonstrate, using FDTD simulation, absorption enhancements in 200nm thick crystalline silicon solar cells of up to 205% from λ = 300nm to 1100nm compared to a planar cell with an optimized two-layer anti-reflection coating. We report here a method to further enhance absorption by introducing a lattice of coupled defect modes into the photonic crystal, which modify the available optical states in the absorber. Our results show that 2D photonic crystals are a viable and rich research option for light trapping in thin film photovoltaics.

Keywords: photonic crystals, defect, silicon, solar cell, absorption, thin-film

1. INTRODUCTION

In silicon photovoltaics, the wafer is currently the dominating factor in module cost. Improved light-trapping within the solar cell can allow for the creation of thinner devices employing less costly semiconductor material while still absorbing a broad spectrum of sunlight and thus maintaining competitive efficiences. In addition to this, the short collection lengths in thinner devices can relax material quality constraints.

It has recently been demonstrated that texturing solar cells with features on the order of the wavelength could potentially allow for absorption the traditional ray optic light trapping limit or the Ergodic limit by enhancing the density of optical states[1,2]. This is due to the fact that a properly nanostructured device can have an elevated local density of optical states (LDOS), allowing for more energy to be in-coupled as well as increasing the light-matter interaction in the solar cell via enhanced electric field in the device, leading to higher absorption. Nanostructures that have been previously explored for light-trapping in solar cells include nanowires[3,4], nanospheres[5], nanodomes[6], photonic crystals[7,8] and plasmonic structures[9]. We focus on using 2D silicon (Si) photonic crystals (PhCs) as the active layer of the solar cell due to their ability to sculpt the photonic bandstructure or available optical modes over a given bandwidth. 2D PhCs also have a simple structure and thus can be fabricated with relative ease on a large-scale using nanoimprint lithography techniques.

We aim to obtain general design principles for photonic crystal solar cells which, despite numerous previous works, have not been clearly identified, and realize the full potential of these structures. We first investigate and optimize defect-free 2D PhC slabs for thin film solar cells with hexagonal and rectangular lattices, then introduce the concept of using sublattices of defects to further enhance absorption. We find that several different defect configurations can lead to small increases absorption compared to the optimal, defect-free case, and that these coupled defects modify not only the available states within the bandgap of the original order crystal, but also give rise to an entirely different set of modes in the bandwidth of interest.

*kwhitese@caltech.edu; phone 626 395-3995; http://daedalus.caltech.edu

Physics, Simulation, and Photonic Engineering of Photovoltaic Devices II, edited by Alexandre Freundlich, Jean-Francois Guillemoles, Proc. of SPIE Vol. 8620, 86200D · © 2013 SPIE
CCC code: 0277-786X/13/$18 · doi: 10.1117/12.2005450

2. ORDERED PHOTONIC CRYSTALS

In this work, "ordered" refers to traditional 2D PhCs with unperturbed in plane periodicity, identical elements in each unit cell, and which have no variation in the out of plane direction. Studying ordered structures provides essential insights into the physics and is the first step towards understanding design of photonic crystal solar cells with additional elements of complexity, such as those incorpating defect modes. We explore the two most common lattice types, square and hexagonal. The four simplest solar cell structures based on these two lattice types are shown in Figure 1. We began by sweeping *r* and *a* for each of the PhCs shown in Figure 1 for *h* = 100nm and 200nm and calculating the integrated absorption spectrally weighted by the solar spectrum to obtain a current, *J*, in units of mA/cm^2. All simulations were performed between wavelengths of 300nm and 1100nm using the Finite Difference Time Domain (FDTD) method. This bandwidth was chosen based on the solar spectrum as well as the electronic band gap of silicon. Bloch boundary conditions were employed in the *xy* plane and the solar cell was considered to be infinite in the *x* and *y* directions.

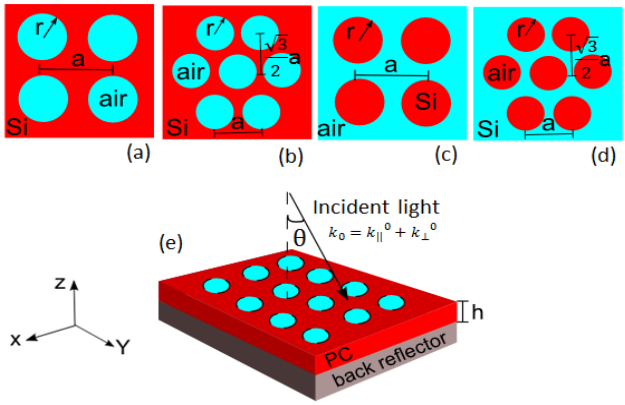

Figure 1. Ordered photonic crystal geometries and coordinate systems used throughout this work.

Figure 2 shows the results of the *r* and *a* optimizations for the four different configurations shown above without a back reflector. For each case, *r* and *a* were each swept from 0 to 700nm in 50nm increments. The maximum *J* was 13.20 mA/cm^2 for the square lattice of air holes in Si, 12.47 mA/cm^2 for the hexagonal lattice of air holes in Si, 10.80 mA/cm^2 for the hexagonal lattice of Si rods in air, and 12.06 mA/cm^2 for the rectangular lattice of Si rods ina ir. This corresponds to an enhancement of 1.96, 1.85, 1.60, and 1.79 times respectively over a planar Si solar cell of the same thickness with an optimized two-layer antireflection coating (ARC) of SiO2 and Si3N, referred to as the reference cell for the remainder of this work. The absorption for all cases of photonic crystal solar cells without a back reflector also surpassed absorption in the planar cells with the optimized two-layer ARC and a perfect backreflector. PhC solar cells comprised of Si rods in air consistently performed worse than Si slabs with holes. This is discussed in detail later on in this section.

Several interesting trends emerged from the *r* and *a* sweeps, which were common to all four structures both with and without employment of a back reflector. First, we note that there are *r/a* ratios, seen as slopes of color in Figure 2, which are better than others over a range of *r* and *a* values. To understand the reasons behind these differences, we examined the modal *E* and *H* profiles for different cases, and similated the in-plane photonic bandstructures for the PhCs in MIT Photonic Bands (MPB), a software program which solves for the definite-frequency eigenstates of Maxwell's Equations. For small *r/a* ratios between 0.1 and 0.2, we found that the in-plane band gap disappears entirely for all simulated cases. For small *r/a*, increased geometric fill factor of the Si, in the case of the holes, or air, in the case of the rods, causes incident waves to see the solar cell more like a homogenous media; in fact, as *r/a* decreases, *J* converges to that of a planar Si slab for air holes in Si and to 0 mA/cm^2 for rods of Si in air. When both *r* and *a* are much smaller than the wavelength, even if *r/a* is large, the wave also does not appear to "see" the periodicity and the material acts as an effective media. Performance was also reduced as *r* and *a* are both increased. In this case, the reduction is due to the fact that as the periodicity and size of the unit cells increase the bandstructure shifts to lower energies or longer wavelengths beyond the electronic band gap of Si. We also performed the same optimizations for a 100nm thick slab and found the same optimal *r* and *a* values as for the 200nm thick case.

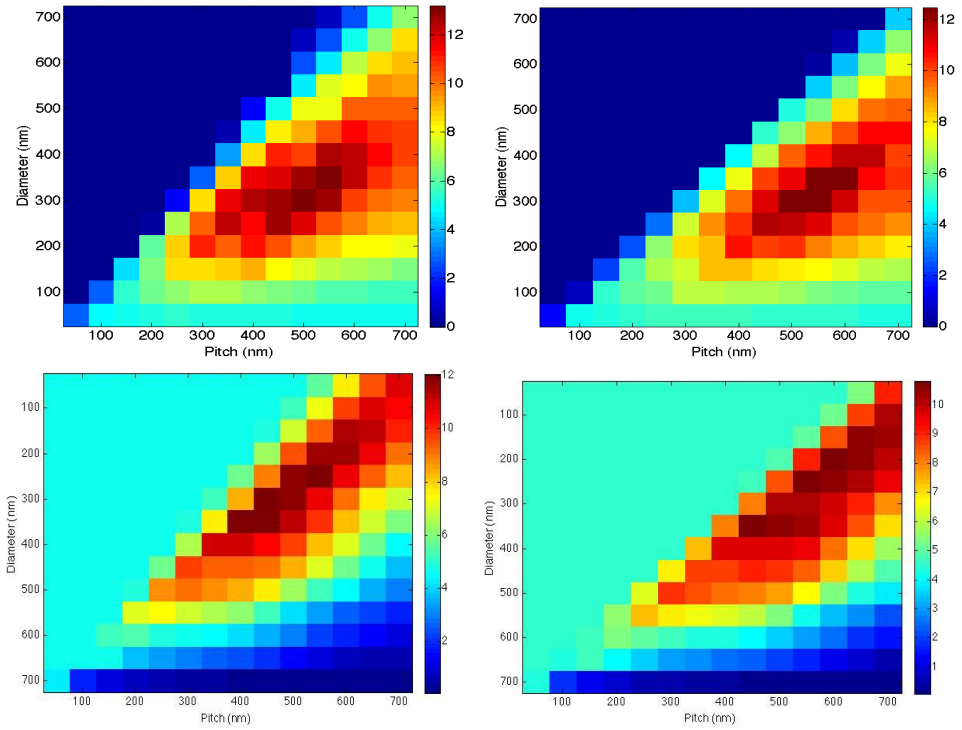

Figure 2. FDTD sweeps for (top left) a rectangular lattice of air holes in Si, (top right) a hexagonal lattice of air holes in Si, (bottom left) a rectangular lattice of Si rods in air, and (bottom right) a hexagonal lattice of Si rods in air

We observed that the optimal *r/a* ratio as well and absolute *r* and *a* values for both lattice types were similar. Table 1 shows the optimal parameters obtained from our simulation as well as results from several other works in the literature. Interestingly, our results are very similar to optimum values reported in the literature where photonic crystals are used as solar cells even when the material and overall geometry of the problem is different from that explored in this work. This suggests that photonic features of the sizes listed in Table 1 are the best for interacting with the spectral region where there is the most power available from the sun at AM 1.5, from about λ = 300nm to the electronic band edge of the material, E_g. The variations for different materials where the active layer is textured can be correlated to the differences in E_g. A larger E_g, for example, would mean that enhancements should be centered at a higher energy where the material can absorb photons. Since *a* shifts the position PhC bands up or down in energy, this would correspond to decreasing *a*. This change in properties of the in-plane, 2D bandstructure is also reflected in the absorption spectra, as can be seen in Figure 3, where the peaks are blue-shifted for small *a* values and red-shifted for larger ones. Figure 3 demonstrates the impacts on the spectra of adjusting *r* around the optimal value, showing a red-shifting of peaks for smaller *r* values with a fixed *a*. Finally, we can observe from this figure that the optimal spectrum has peaks that are neither the broadest nor the most narrow.

The enhancements seen in the blue region of the spectrum are mostly due to an anti-reflection effect, as articulated in Figure 3. In these spectral regions, the interaction with leaky photonic modes is much weaker, and the strong single pass absorption of Si dominates. For different photonic structures the absorption peaks are similar, but the magnitude of absorption is increased proportional to the ratio of air to Si in the photonic crystal or inversely proportional to the average effective index, consistent with an anti-reflection effect.

Absorption enhancements were robust to variation. Roughening the unit cell holes with three different random rough surfaces, for example, changed J by less than 0.8 mA/cm^2. However, changing the shape of the air holes or rods to squares and triangles significantly changed the spectral response. Still, the integrated absorption enhancements compared to the flat cell with optimized two-layer ARC remained greater than unity for all cases, being 1.70 and 1.87 for the shapes respectively for *a* = 550nm and hole size 350 nm for cells without a back reflector.

Table 1. Comparison of our simulated results to literature values. * indicates a result from this work.

Optimal *r* (nm)	Optimal *a* (nm)	Optimal *r/a*	Materials	Thickness	Lattice type	Source
175	550	0.318	air holes in a c-Si slab	100nm, 200nm	Square	*
150	500	0.3039	air holes in a c-Si slab	100nm, 200nm	Hexagonal	*
198	600	0.33	holes filled withof n = 1.65 in c-Si slab	190nm PhC on a 1μm slab	Square	[10]
150	470	0.32	air holes in InP and unspecified ARC layers	varied	Hexagonal	[11]
110	400	0.275	TDPTD:PhCBM with nc-ZnO filled holes	180nm	Hexagonal	[12]
155	620	0.25	c-Si with Ag grating at back	> 5μm Si cell	Square	[13]

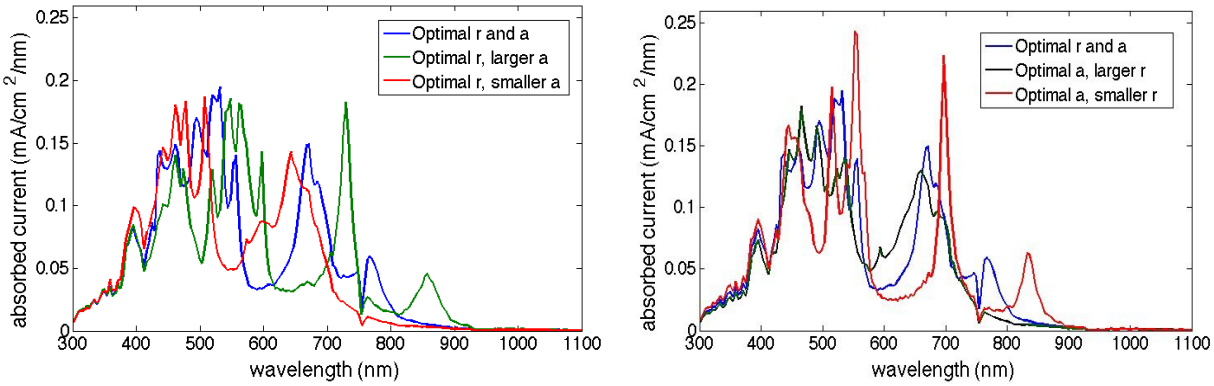

Figure 3. Spectrum for the highest performing hexagonal lattice, a = 500nm and r = 150nm, as well as spectra for cases where (left) a is varied around the optimal point and (right) r is varied around the optimal point.

The angular response of the ordered rectangular lattice with *a* = 500nm and r = 175 nm is shown below in Figure 4. We observed that the change in absorption spectrum with angle followed the bandstructure of the photonic crystal in *k*-space well. It is exciting to note that, while there is variation in the spectrum with angle, there are many modes which appear flat, existing for all angles, particularly for the TM polarized light. This means our designs show a angularly robust enhancements at long-wavelengths near the electronic band edge of Si where the material is naturally weakly absorbing.

The angle sweeps were performed using rigorous coupled-wave analysis (RCWA) rather than FDTD due to the long computation times required to complete these simulation in FDTD. Test points from these sweeps were selected and additionally simulated in FDTD to verify results. Indeed, the results from RCWA agreed well with results obtained using the FDTD method used elsewhere in this work.

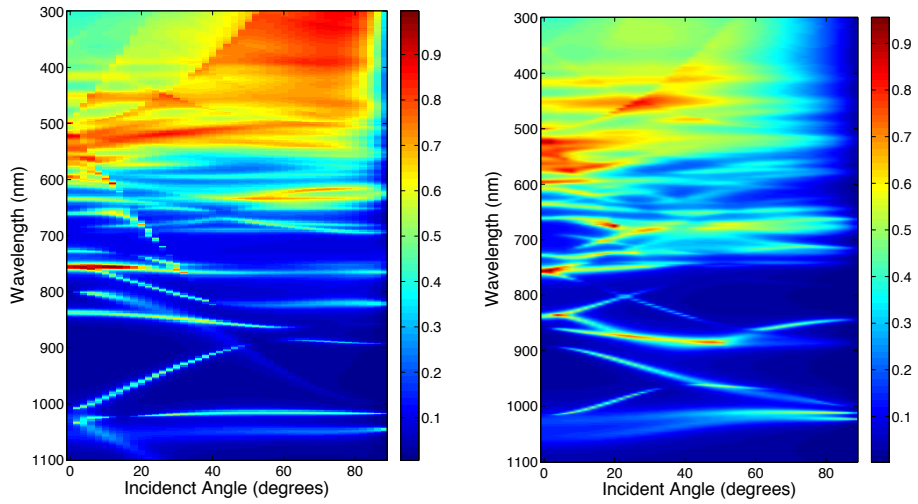

Figure 4. Angular spectrum for a rectangular lattice of air holes in Si with a = 500nm and r = 175nm for (left) TM polarization and (right) TE polarization. The color bar represents normalized absorption.

3. INTRODUCING DEFECT MODES

Defects breaking of the original periodicity in a photonic crystal and thus introduce new modes. If the defects are not close packed, i.e. are either uncoupled or weakly coupled, these new modes are introduced into the bandgaps of the photonic crystal and enhance the density of states over a certain spectral range. For tightly coupled, close-packed defects as explored in this initial work, the defects may instead create a sublattice and give rise to an entirely new bandstructure. Since the latter case allows for periodic simulations with a small periodicity, they are more ammenable to FDTD simulation than the former case.

We investigated the impact of adding defect modes to the optimized ordered crystal, as determined in Section 2, with a = 550nm and r = 350nm. Figure 5 shows the variation in J with defect diameter for three different arrangements of defects. As can be seen from the plot, the addition of defects improves J for some defects with diameters similar to those of the ordered base lattice, but actually decreases it for other defect sizes. These changes could be due to several factors, including enhanced or weakened electric field in the defect area, constructive or destructive interference between neighboring defect resonances, or creation of an entirely different bandstructure with a different density of states in the case of very closely packed defects.

To examine some of the defect modes more closely we plot field profiles for specific wavelengths with and without a defect in Figure 6. The top row in Figure 6 shows the electric field intensity profiles for an ordered lattice and a lattice with a 0 nm center defect. The intensity is greatly increased for the defect mode, which leads to higher absorption at this wavelength. It can also be seen that the field profile is perturbed by the addition of the defect. The new profile suggests that there is a new propagating mode at this frequency. This can be explained by considering the defects as a coupled chain of resonators due to their fields overlapping because of their close proximity to each other. The bottom row shows the magnetic field profiles with and without the defect. Again, a greater intensity is achieved with the defect and the field profile is changed by the presence of the defect.

The defect structure for which the highest current was obtained is a close packed edge-defect arrangement with defect diameter of 300nm. While the current for this case, 13.8 mA/cm^2 , represents a fairly small enhancement compared to the defect-free case, it is nonetheless notable given that the optimal ordered lattice does not in fact have a complete bandgap for either the TE or the TM mode within the bandwidth of interest (λ = 300nm to 1100nm).

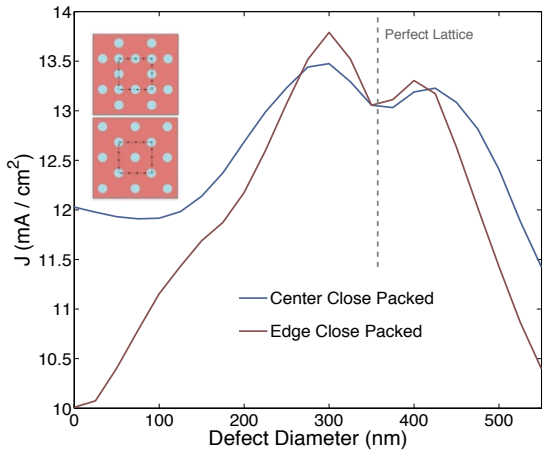

Figure 5. Changes in J with defect diameter for center close packed (top) and edge close packed (bottom) for a lattice with a = 550nm and d = 350nm.

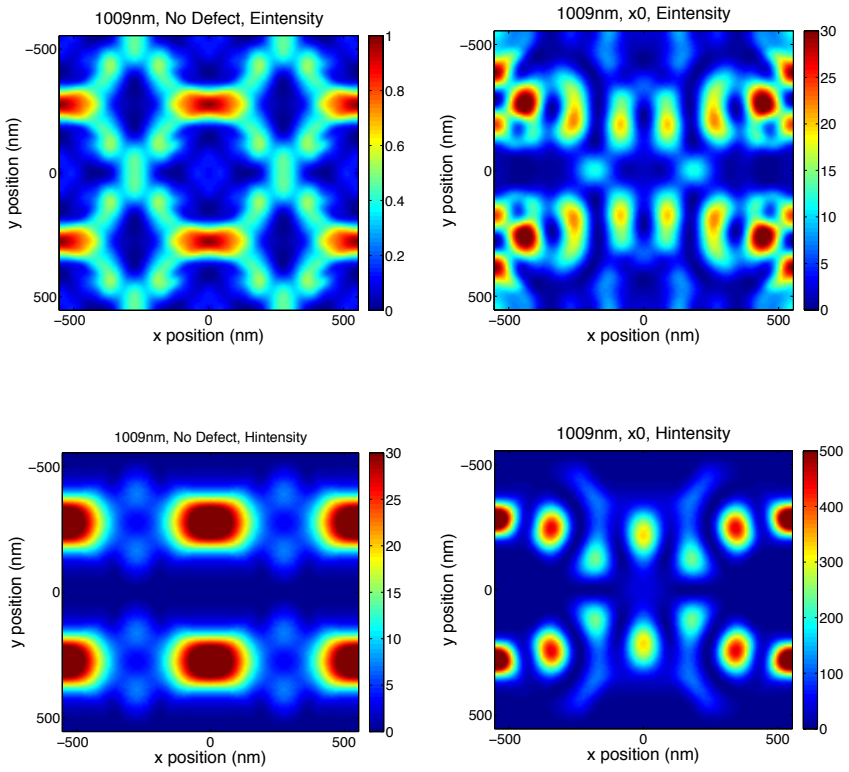

Figure 6. (top row) Electric field intensity profiles at 1009nm for ordered lattice (left) and lattice with 0nm center defect (right). (bottom row) Magnetic field intensity profiles for ordered lattice (left) and lattice with 0nm center defect (right).

4. CONCLUSION

We have explored various geometries for periodically texturing thin film Si to increase light trapping. We optimized lattice period and feature diameter for four different lattices and have shown that the optimized absorbed current is higher than a planar Si slab with a double layer AR coating for all lattice types. We investigated by the optimal ordered lattice further by roughening and changing the shape of the features and by calculating the behavior at varying incident angles. We improved the absorbed current for the optimal lattice by introducing sublattices of defects into the ordered lattice and optimizing the defect size. We find that at frequencies where the defects introduce new resonances to the photonic crystal there is a perturbed electric field profile and an increased field intensity, leading to higher absorption at the resonant frequencies.

ACKNOWLEDGEMENTS

This work was supported by the Bay Area Photovoltaics Consortium and the Caltech-Taiwan Energy Exchange program through National Central University; Kelsey A. Whitesell also acknowledges fellowship support from the National Science Foundation Graduate Research Fellowship program.

REFERENCES

[1] Yu, Z., Raman, A., and Shanhui, F. "Fundamental limit of nanophotonic light trapping in solar cells," PNAS 107(41), 17491-17496 (2010).
[2] Callahan, D. M., Munday, J.N., and Atwater, H.A. "Solar cell light trapping beyond the ray optic limit," Nanoletters 12(1), 214-218 (2012).
[3] Garnett, E. and Yang, P. "Light trapping in silicon nanowire solar cells," Nanoletters 10(3), 1082-1087 (2010).
[4] Kelzenberg, M.D, Turner-Evans, D.B., Kayes, B.M., Filler, M.A., Putnam, M.C., Lewis, N.S., and Atwater, H.A. "Photovoltaic measurements in single-nanowire silicon solar cells," Nanoletters 8(2), 710-714 (2008).
[5] Grandidier, J., Callahan, D.M., Munday, J.N., and Atwater, H.A. "Light absorption enhancement in thin-film solar cells using whispering gallery modes in dielectric nanospheres," Advanced Materials 23(10), 1272-1276 (2011).
[6] Zhu, J., Hsu, C.M, Yu, Z., Fan, S., and Cui, Y. "Nanodome solar cells with efficient light management and self-cleaning," Nanoletters 10(6), 1979-1984 (2010).
[7] Bermel, P., Luo, C., Zeng, L., Kimerling, L.C., and Joannopoulos, J.D. "Improving thin-film crystalline silicon solar cell efficiencies with photonic crystals," Optics Express 15(25), 16986-17000 (2007).
[8] Chutinan, A., Kherani, N.P, and Zukotynski, S. "High-efficiency photonic crystal solar cell architecture," Optics Express 17(11), 8871-8878 (2009).
[9] Catchpole, K.R. and Polman, A. "Plasmonic solar cells," Optics Express 16(26), 21793-21800 (2008).
[10] Bozzola, A., Liscidini, M., and Andreani, L.C. "Photonic light-trapping versus Lambertian limits in thin film silicon solar cells with 1D and 2D periodic patterns," Optics Express 20(S2), A224-A244 (2012).
[11] Postigo, P.A. "Solar-cell efficiency enhancements using 2D photonic crystals," SPIE Newsroom (2010).
[12] Ko, D.H., Tumbleston, J.R., Zhang, L., Williams, S., DeSimone, J.M., Lopez, R., and Samulski, E.T. "Photonic crystal geometry for organic solar cells," Nanoletters 9(7), 2742-2746 (2009).
[13] Heine, C. and Morf, R.H. "Submicrometer gratings for solar energy applications," Applied Optics 34(14), 2476-2482 (1995).